Received: 16 December 2021 | Revised: 3 May 2022 | Accepted: 24 May 2022

DOI: 10.1002/jsp2.1210

RESEARCH ARTICLE

JOR Spine OPEN ACCESS

Comparative proteome analysis of the ligamentum flavum of patients with lumbar spinal canal stenosis

Yutaka Yabe[1] | Yoshihiro Hagiwara[1] | Masahiro Tsuchiya[2] | Takashi Minowa[3] | Taro Takemura[3] | Shinya Hattori[3] | Shinichirou Yoshida[1] | Takahiro Onoki[1] | Keisuke Ishikawa[1]

[1]Department of Orthopaedic Surgery, Graduate School of Medicine, Tohoku University, Sendai, Japan

[2]Department of Nursing, Faculty of Health Science, Tohoku Fukushi University, Sendai, Japan

[3]Nanotechnology Innovation Station, National Institute for Materials Science, Tsukuba, Japan

Correspondence
Yutaka Yabe, Department of Orthopaedic Surgery, Graduate School of Medicine, Tohoku University, 1-1 Seiryo-machi, Aoba-ku, Sendai 980–8574, Japan.
Email: yabe@med.tohoku.ac.jp

Funding information
Ministry of Education, Culture, Sports, Science and Technology, Grant/Award Number: JPMXP09 S20NM0025

Abstract

Background: Thickening of the ligamentum flavum is considered to be the main factor for lumbar spinal canal stenosis (LSCS). Although some mechanisms have been speculated in the thickening of the ligamentum flavum, there are only a few comprehensive approaches to investigate its pathology. The objective of this study was to investigate the pathology of thickened ligamentum flavum in patients with LSCS based on protein expression levels using shotgun proteome analysis.

Methods: Ligamentum flavum samples were collected from four patients with LSCS (LSCS group) and four patients with lumbar disc herniation (LDH) as controls (LDH group). Protein mixtures were digested and analyzed by liquid chromatography/mass spectrometry analysis. To compare protein expression levels between the LSCS and LDH groups, the mean Mascot score was compared. Biological processes were assessed using Gene Ontology analysis.

Results: A total of 1151 proteins were identified in some samples of ligamentum flavum. Among these, 145 proteins were detected only in the LSCS group, 315 in the LDH group, and 691 in both groups. The demonstrated biological processes occurring in the LSCS group included: extracellular matrix organization, regulation of peptidase activity, extracellular matrix disassembly, and negative regulation of cell growth. Proteins related to fibrosis, chondrometaplasia, and amyloid deposition were found highly expressed in the LSCS group compared with those in the LDH group.

Conclusions: Tissue repair via fibrosis, chondrometaplasia, and amyloid deposits may be important pathologies that occur in the thickened ligamentum flavum of patients with LSCS.

KEYWORDS
amyloid, chondrometaplasia, fibrosis, ligamentum flavum, lumbar spinal canal stenosis, proteome analysis, thickening

1 | INTRODUCTION

Lumbar spinal canal stenosis (LSCS) is one of the most common spinal disease among elderly people.[1] Thickening of the ligamentum flavum, which covers the posterior and lateral walls of the spinal canal, is considered the main causative factor in LSCS.[2] The ligamentum flavum is a yellow-colored ligament connecting the upper and lower vertebrae.[3] It is abundant in elastic fibers, providing elasticity, which is different

from other ligaments that are mainly comprised of collagen fibers.[4] Thickening of the ligamentum flavum has been reported as caused by tissue hypertrophy and buckling of the ligament.[5,6] Previous studies have shown that a thickened ligamentum flavum contains decreased elastic fibers and increased collagen fibers.[7,8] Fibrosis is considered the main pathology in ligamentum flavum thickening.[9] Furthermore, some authors have indicated that chondrometaplasia and inflammation are detected in thickened ligamentum flavum.[2,5,10] Although some mechanisms have been speculated in thickening of the ligamentum flavum, there are only a few comprehensive approaches to investigate its pathology.

Shotgun proteome analyses via liquid chromatography tandem mass spectrometry (LC/MS/MS) is a powerful method to comprehensively detect proteins and elucidate the mechanisms of disease.[11] Messenger RNA expression levels have been commonly used to assess thickened ligamentum flavum; however, they sometimes have weak correlations with protein expression levels.[12] Furthermore, LSCS is a disease with a long duration and ligamentum flavum hypertrophy is considered to occur with instability of the lumbar spine, which is a precursor to disc collapse.[6,8,13] Thickened ligamentum flavum can be already hypertrophied, and not just hypertrophying.[14] Therefore, proteome analysis is important to understand the pathology of the disease. The aim of this study was to investigate the pathology of thickened ligamentum flavum based on protein expression levels using shotgun proteome analysis.

2 | MATERIALS AND METHODS

2.1 | Patients and tissue collection

This study was reviewed and approved by the institutional review board of our university (approval number: 2017-1-348). The ligamentum flavum of eight patients requiring decompressive surgery was obtained for proteomic analyses. Among these, four samples were from patients with LSCS and thickening of the ligamentum flavum on magnetic resonance imaging (MRI). These comprised the study group (LSCS group). The other four samples were from patients with lumbar disc herniation (LDH) without thickening of the ligamentum flavum on MRI. These comprised the control group (LDH group). Neither group included patients on hemodialysis. The thickness of the ligamentum flavum was assessed using MRI as previously reported and the maximum thickness of the ligamentum flavum was measured at the facet joint level on axial T1-weighted imaging.[4] The ligamentum flavum was considered thickened if it had more than 4 mm of thickness on MRI in accordance with a previous report.[15] The list of patients is shown in Table 1. The average age of the LSCS group (two men and two women) patients and that of the LDH group (two men and two women) was 70.8 years (range, 63–75 years; SD, 5.4 years) and 58 years (range, 45–64 years; SD, 8.6 years), respectively. The mean thickness of the ligamentum flavum was 4.72 mm (range, 4.15–5.53; SD, 0.59 mm) in the LSCS group and 2.75 mm (range, 1.99–3.54; SD, 0.63 mm) in the LDH group.

2.2 | Sample preparation for comparative proteomics

Ligamentum flavum samples were obtained en-bloc during surgery and immediately snap-frozen in liquid nitrogen, and the following

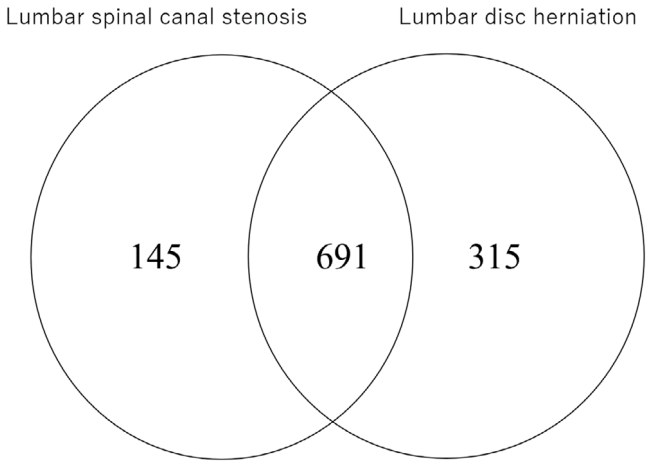

FIGURE 1 Venn diagram of ligamentum flavum proteins in lumbar spinal canal stenosis vs lumbar disc herniation. Expressed protein numbers per group is in tables

TABLE 1 List of patients

		Age	Sex	Comorbidity	Ligamentum flavum thickness (mm)
LSCS	1	63	Female	Breast cancer	4.45
	2	71	Male	—	4.15
	3	74	Female	HT	5.53
	4	75	Male	HT, angina pectoris	4.73
LDH	1	45	Male	Gastric cancer	1.99
	2	61	Female	HT, HL	2.75
	3	62	Female	HT, cerebellar infarction	2.7
	4	64	Male	HT, HL, DM	3.54

Abbreviations: DM, diabetes mellitus; HL, hyperlipidemia; HT, hypertension; LDH, lumbar disc herniation; LSCS, lumbar spinal canal stenosis.

detailed procedures and analyses were performed for each sample. Samples were initially homogenized using a FastPrep machine, followed by sequential extraction. To reduce the complexity of each extracted fraction, Sodium dodecyl sulfate-polyachrylamide gel electrophoresis (SDS-PAGE)-based protein fractionation was performed using the GELFREE 8100 fractionation system (Expedeon, Heidelberg, Germany). Fractionation conditions of the GELFREE 8100 system were described elsewhere.[16] To remove the detergent from each fraction, the solution was treated with Pierce™ Detergent removal spin column (Thermo Fisher Scientific, Waltham, MA, USA), then was further treated with HiPPR™ detergent removal resin (Thermo Fisher Scientific). The detailed steps for protein extraction, fractionation, and digestion are shown in Data S1.

2.3 | Liquid chromatography/mass spectrometry measurement

Liquid chromatography/mass spectrometry analysis was performed using a nanoadvance LC system (Bruker Daltonics, Bremen, Germany) interfaced with a Q-Exactive Plus Orbitrap mass spectrometer (Thermo Fisher Scientific) via an Advance Captive Spray ionization source (AMR, Tokyo, Japan). Digested peptides were loaded onto a trap column (L-column ODS 5 μm, Chemical Evaluation and Research Institute Japan, Tokyo, Japan) with Buffer A for concentration and desalting. Subsequently, samples were eluted from the trap column and the analytical column (Zaplous α-Pep C18 nano HPLC column, AMR) with a linear gradient of Mobile

TABLE 2 Major proteins in the ligamentum flavum

Accession	Description	Mean Mascot score
P51888	Prolargin OS = Homo sapiens GN = PRELP PE = 1 SV = 1	24 862
P04264	Keratin, Type II cytoskeletal 1 OS = Homo sapiens GN = KRT1 PE = 1 SV = 6	21 419
P10909	Clusterin OS = Homo sapiens GN = CLU PE = 1 SV = 1	16 628
P51884	Lumican OS = Homo sapiens GN = LUM PE = 1 SV = 2	10 904
P02743	Serum amyloid P-component OS = Homo sapiens GN = APCS PE = 1 SV = 2	10 529
P35527	Keratin, Type I cytoskeletal 9 OS = Homo sapiens GN = KRT9 PE = 1 SV = 3	10 519
P13645	Keratin, Type I cytoskeletal 10 OS = Homo sapiens GN = KRT10 PE = 1 SV = 6	10 024
P08670	Vimentin OS = Homo sapiens GN = VIM PE = 1 SV = 4	9665
P35908	Keratin, Type II cytoskeletal 2 epidermal OS = Homo sapiens GN = KRT2 PE = 1 SV = 2	8823
P01857	Ig gamma-1 chain C region OS = Homo sapiens GN = IGHG1 PE = 1 SV = 1	8728
P02766	Transthyretin OS = Homo sapiens GN = TTR PE = 1 SV = 1	7908
P20774	Mimecan OS = Homo sapiens GN = OGN PE = 1 SV = 1	7769
O75339	Cartilage intermediate layer protein 1 OS = Homo sapiens GN = CILP PE = 1 SV = 4	7399
P04259	Keratin, Type II cytoskeletal 6B OS = Homo sapiens GN = KRT6B PE = 1 SV = 5	6829
P08779	Keratin, Type I cytoskeletal 16 OS = Homo sapiens GN = KRT16 PE = 1 SV = 4	6514
P02533	Keratin, Type I cytoskeletal 14 OS = Homo sapiens GN = KRT14 PE = 1 SV = 4	6428
P07585	Decorin OS = Homo sapiens GN = DCN PE = 1 SV = 1	6416
P21810	Biglycan OS = Homo sapiens GN = BGN PE = 1 SV = 2	6228
Q9BXN1	Asporin OS = Homo sapiens GN = ASPN PE = 1 SV = 2	5798
P01834	Ig kappa chain C region OS = Homo sapiens GN = IGKC PE = 1 SV = 1	5371
P01859	Ig gamma-2 chain C region OS = Homo sapiens GN = IGHG2 PE = 1 SV = 2	5330
P01860	Ig gamma-3 chain C region OS = Homo sapiens GN = IGHG3 PE = 1 SV = 2	5256
P02647	Apolipoprotein A-I OS = Homo sapiens GN = APOA1 PE = 1 SV = 1	4588
P08294	Extracellular superoxide dismutase [Cu-Zn] OS = Homo sapiens GN = SOD3 PE = 1 SV = 2	4509
Q92743	Serine protease HTRA1 OS = Homo sapiens GN = HTRA1 PE = 1 SV = 1	4383
P48668	Keratin, Type II cytoskeletal 6C OS = Homo sapiens GN = KRT6C PE = 1 SV = 3	4302
P06727	Apolipoprotein A-IV OS = Homo sapiens GN = APOA4 PE = 1 SV = 3	4285
P19012	Keratin, Type I cytoskeletal 15 OS = Homo sapiens GN = KRT15 PE = 1 SV = 3	4143
P02538	Keratin, Type II cytoskeletal 6A OS = Homo sapiens GN = KRT6A PE = 1 SV = 3	4139
Q04695	Keratin, Type I cytoskeletal 17 OS = Homo sapiens GN = KRT17 PE = 1 SV = 2	4138
P00738	Haptoglobin OS = Homo sapiens GN = HP PE = 1 SV = 1	4115
P08727	Keratin, Type I cytoskeletal 19 OS = Homo sapiens GN = KRT19 PE = 1 SV = 4	4002

phase B from 5% to 45% in 20 min at a flow rate of 500 nl/min (Mobile phase A: 99.9% distilled water and 0.1% formic acid; Mobile phase B: 100% acetonitrile). Acquiring MS spectrum parameters were set as follows: electrospray voltage, 1.8 kV; temperature of the ion transfer tube, 150°C; collision energy, 27; threshold of ion selection for MS/MS, 1700 count; mass range at 350 to 2000 m/z, resolution at 70000, and a maximum acquisition time of 60 ms. MS/MS scanning was performed on the top 10 abundant precursor ions with dynamic exclusion for 20 s after selection. Each sample was measured three times.

2.4 | Data analysis for protein identification

The raw data were analyzed automatically using Proteome discoverer 2.0 software (Thermo Fisher Scientific) with in house Mascot v.2.5 search engine (Matrix Science, London, UK) and the SwissProt database of Homo sapiens (UniProt, Geneva, Switzerland) with the following parameters: maximum missed cleavage sites, 2; instrument type; ESI-TRAP, precursor mass tolerance, 10 ppm; fragment mass tolerance, 0.02 Da; dynamic modifications, methionine oxidation, static modification, and cysteine carbamidomethyl. All proteins were identified with a false discovery rate of <1% based on a decoy database search. For the analysis of 1 patient, a total of 60 raw data points (including 2 types of extraction, 5 fractions, 2 types of detergent removal, and 3 measurements) were combined for the analysis. Proteins with a Mascot score >30 are listed. To compare the protein expression levels between the LSCS and LDH groups, the mean and SD of the Mascot score were calculated and compared. Biological processes were assessed using Gene Ontology (GO) analysis.

TABLE 4 Characteristic biological events increased in the LSCS group

Term	Genes
GO:0030198 ~ extracellular matrix organization	P02766, P02751, P49747
GO:0048048 ~ embryonic eye morphogenesis	Q12805, O15169
GO:0010952 ~ positive regulation of peptidase activity	Q9UKZ9, P02751
GO:0001523 ~ retinoid metabolic process	P06727, P02766
GO:0022617 ~ extracellular matrix disassembly	P02751, Q92743
GO:0002576 ~ platelet degranulation	P04196, P02751
GO:0044267 ~ cellular protein metabolic process	P06727, P02766
GO:0030308 ~ negative regulation of cell growth	P07093, P04196
GO:0010951 ~ negative regulation of endopeptidase activity	P07093, P04196

Abbreviation: LSCS, lumbar spinal canal stenosis.

TABLE 3 The proteins found increased in the LSCS group

		Mascot score				
		LDH		LSCS		
Accession	Description	Mean	SD	Mean	SD	LSCS/LDH
P07093	Glia-derived nexin OS = Homo sapiens GN = SERPINE2 PE = 1 SV = 1	–		193	138	–
P02748	Complement component C9 OS = Homo sapiens GN = C9 PE = 1 SV = 2	156	63	1500	1071	9.6
P02766	Transthyretin OS = Homo sapiens GN = TTR PE = 1 SV = 1	1574	538	14 242	10 281	9.0
Q96DN6	Methyl-CpG-binding domain protein 6 OS = Homo sapiens GN = MBD6 PE = 1 SV = 2	38	6	206	238	5.4
Q9UKZ9	Procollagen C-endopeptidase enhancer 2 OS = Homo sapiens GN = PCOLCE2 PE = 1 SV = 1	125	75	576	227	4.6
Q12805	EGF-containing fibulin-like extracellular matrix protein 1 OS = Homo sapiens GN = EFEMP1 PE = 1 SV = 2	66	22	238	215	3.6
P06727	Apolipoprotein A-IV OS = Homo sapiens GN = APOA4 PE = 1 SV = 3	1884	1538	6686	1930	3.5
Q92743	Serine protease HTRA1 OS = Homo sapiens GN = HTRA1 PE = 1 SV = 1	2059	671	6707	2348	3.3
P02751	Fibronectin OS = Homo sapiens GN = FN1 PE = 1 SV = 4	1880	1175	6025	4367	3.2
Q8IUL8	Cartilage intermediate layer protein 2 OS = Homo sapiens GN = CILP2 PE = 2 SV = 2	621	397	1528	1147	2.5
P04196	Histidine-rich glycoprotein OS = Homo sapiens GN = HRG PE = 1 SV = 1	151	50	348	268	2.3
O15169	Axin-1 OS = Homo sapiens GN = AXIN1 PE = 1 SV = 2	47	13	97	37	2.1
P49747	Cartilage oligomeric matrix protein OS = Homo sapiens GN = COMP PE = 1 SV = 2	2469	875	5053	3918	2.0

Abbreviations: LDH, lumbar disc herniation; LSCS, lumbar spinal canal stenosis.

2.5 | Tissue staining

According to the results of the proteome analyses, Elastica-Masson staining, alcian blue staining, and direct fast scarlet staining were used to visualize fibrotic and fibrocartilage changes and amyloid deposition in the ligamentum flavum. Furthermore, the protein expression levels of HTRA serine protease 1 (HTRA1), cartilage intermediate layer protein-2 (CLIP-2), cartilage oligomeric matrix protein (COMP), and transthyretin were visualized using immunohistochemistry. Additional ligamentum flavum samples were obtained during surgery for tissue staining and embedded in paraffin after being fixed with 4% paraformaldehyde in 0.1 M phosphate-buffered saline, pH 7.4. Four samples each were obtained from patients with LSCS and those with LDH. The paraffin-embedded tissue cut into 5-μm sections were deparaffinized and stained. Immunohistochemistry was performed as previously described.[5] The antibodies against HTRA1 (MAB29161, R&D systems, Minneapolis, MN, USA); CLIP-2 (ab224111, Abcam, Cambridge, UK); COMP (ab231977, Abcam); and transthyretin (A0002, DAKO, Santa Clara, CA, USA) were used. Negative control testing was performed using normal rabbit or mouse IgG as the primary antibody. All slides were stained in one session. For quantified analysis of the immunohistochemistry, the regions of interest in an area of 0.25 mm^2 were randomly selected from five sites in each ligamentum flavum sample and the stained area within the region of interest was calculated using ImageJ 1.53 software (National Institutes of Health, Bethesda, MD, USA). Differences between the LSCS and LDH groups were compared by an unpaired *t*-test, and a *p*-value of <0.05 was considered to be statistically significant.

3 | RESULTS

A total of 1151 proteins were identified in some samples of the ligamentum flavum by proteome analysis (Table S1). Among these, 145 proteins were detected only in the LSCS group, 315 only in the LDH group, and 691 in both groups (Figure 1). To investigate common proteins detected in the ligamentum flavum, major proteins with a mean Mascot score of >3000 are listed in Table 2. The protein with

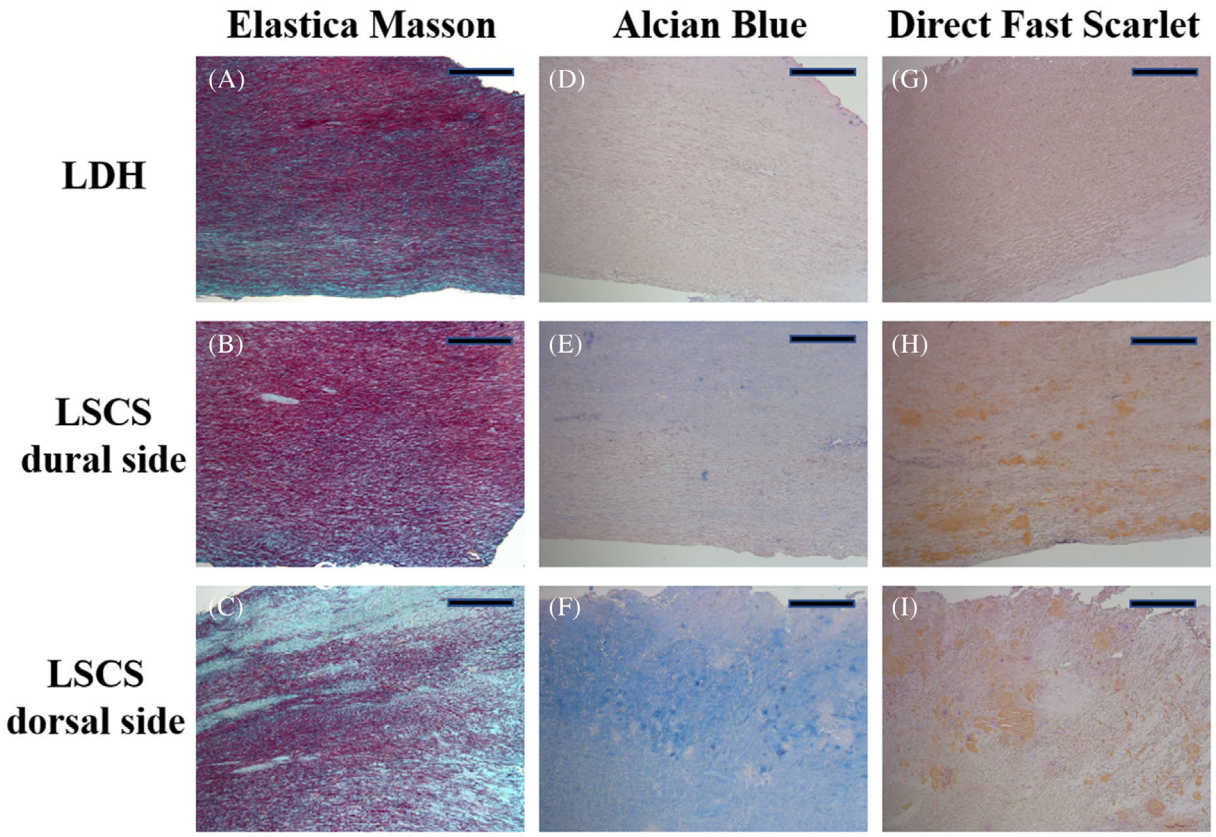

FIGURE 2 Elastica-Masson staining, alcian blue staining, and direct fast scarlet staining of the representative ligamentum flavum tissue. (A) Elastica-Masson staining of the ligamentum flavum in the LDH group; (B) dural side in the LSCS group; (C) dorsal side in the LSCS group; (D) alcian blue staining in the LDH group; (E) dural side in the LSCS group; (F) dorsal side in the LSCS group; (G) direct fast scarlet staining in the LDH group; (H) dural side in the LSCS group; and (I) dorsal side in the LSCS group. Elastic fibers were decreased, and collagen fibers were increased in the LSCS group, especially on the dorsal side. Dark purple and green areas indicate elastic fibers and collagen fibers, respectively (A–C). Intensity of alcian blue staining was strong in the LSCS group, especially on the dorsal side, indicating fibrocartilage changes (D–F). Increased amyloid deposition was observed in both dural and dorsal sides in the LSCS group (G–I). Scale bars: 500 μm. LDH, lumbar disc herniation; LSCS, lumbar spinal canal stenosis.

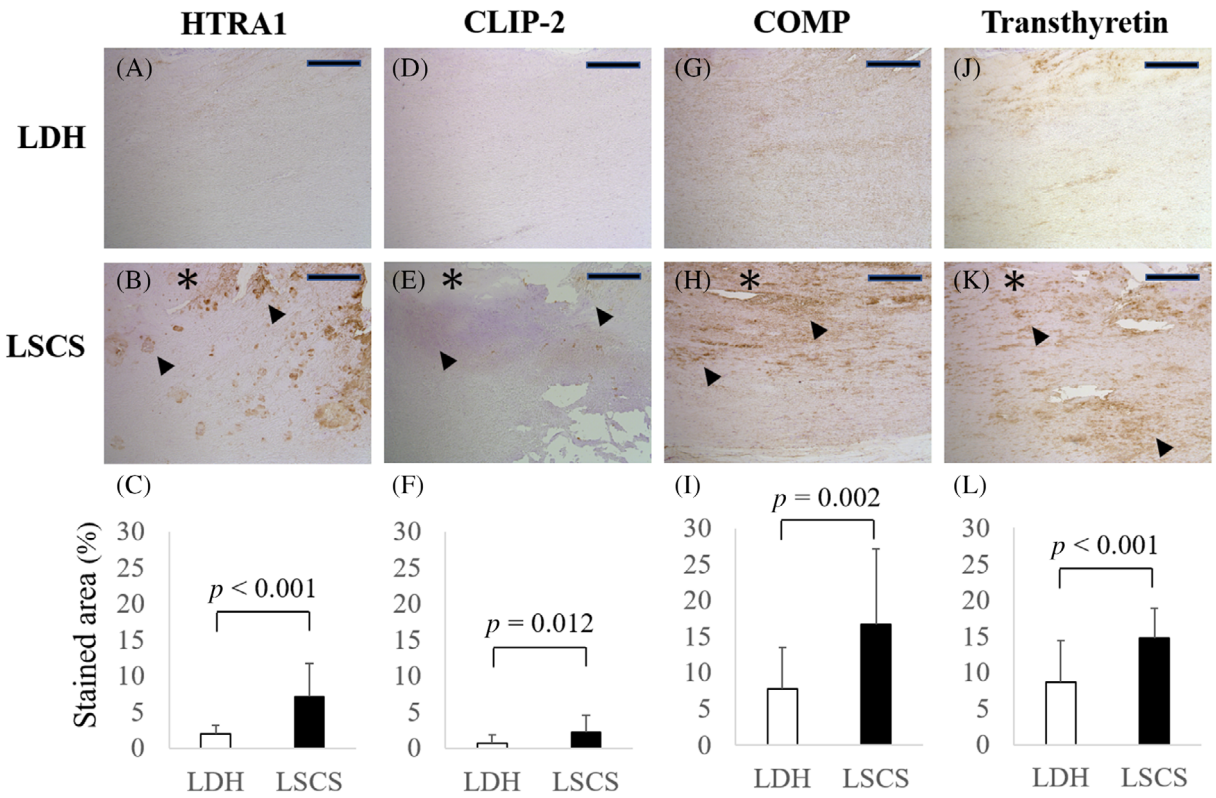

FIGURE 3 Immunostainings of ligamentum flavum. (A) Immunoreactivity of HTRA1 in the LDH group, (B) the LSCS group, and (C) the ratio of the stained area. (D) Immunoreactivity of CLIP-2 in the LDH group, (E) the LSCS group, and (F) the ratio of the stained area. (G) Immunoreactivity of COMP in the LDH group, (H) the LSCS group, and (I) the ratio of stained area. (J) Immunoreactivity of transthyretin in the LDH group, (K) the LSCS group, and (L) the ratio of the stained area. Stronger immunoreactivities of HTRA1, CLIP-2, and COMP, which were stained brown, were observed especially on the dorsal side in the LSCS group. Stronger immunoreactivities of transthyretin, which was stained brown, were detected in both dural and dorsal sides in the LSCS group (A–L). Asterisks indicate the dorsal side, and arrow heads show immunoreactivities of HTRA1 (B), CLIP-2 (E), COMP (H), and transthyretin (K). Data are expressed as means ± SD (C,F,I,L). Scale bars: 500 μm. CLIP-2, cartilage intermediate layer protein-2; COMP, cartilage oligomeric matrix protein; HTRA1, HTRA serine protease 1; LDH, lumbar disc herniation; LSCS, lumbar spinal canal stenosis.

the highest Mascot score was prolargin, which was followed by keratin (Table 2). The proteins increased in the LSCS group are shown in Table 3. A total of 275 proteins were detected in all the samples of the LSCS group. Among these, glia-derived nexin was not detected in the LDH group. Furthermore, 12 proteins showed more than double upregulation rates in the LSCS group compared with those in the LDH group (Table 3). We identified nine GO biological process terms in the LSCS group (Table 4). The proteins found decreased in the LSCS group are shown in Table S2. Among 389 proteins that were detected in all the samples in the LDH group, seven were not detected in the LSCS group and 68 proteins had less than half downregulation rates in the LSCS group compared with those in the LDH group (Table S2). We identified 71 GO biological process terms in the LSCS group (Table S3). Representative ligamentum flavum stained tissues are shown in Figures 2 and 3. In the LSCS group, decreased elastic fibers, increased collagen fibers, and fibrocartilage changes were observed, especially on the dorsal side of the ligamentum flavum. Similarly, amyloid deposition was observed in both dural and dorsal sides of the ligamentum flavum in the LSCS group. Stronger immunoreactivities of HTRA1, CLIP-2, and COMP were detected, especially on the dorsal side of the ligamentum flavum in the LSCS group, while stronger immunoreactivities of transthyretin were observed in both dural and dorsal sides of ligamentum flavum in the LSCS group (Figure 3).

4 | DISCUSSION

The present study investigated protein expression levels in ligamentum flavum samples using proteomic analysis to further understand the pathology of ligamentum flavum hypertrophy. Proteomic analysis is commonly used in the analysis of human tissues.[11,17] However, it is rarely applied to ligaments, especially ligamentum flavum.[18–20] Furthermore, only two reports investigated the pathology of the thickened ligamentum flavum by comparing protein expression levels in the ligamentum flavum of LSCS and LDH patients.[19,20] In one of these reports, there was approximately a 30-year age difference between the two groups of patients, while the other did not include any relevant information. Generally, LSCS patients are older

than LDH patients, and the difference in age is a limitation of the method that used the ligamentum flavum of LDH patients as a control. In the current study, the age difference between the two groups was 13 years, which was smaller than that of the previous report, making the effect of aging less significant.

Among the proteins detected in ligamentum flavum tissue with high expression levels by proteomic analysis, the characteristic proteins were prolargin, lumican, mimecan, decorin, biglycan, asporin, and fibromodulin. These proteins belong to the small leucine-rich proteoglycan family, which maintains extracellular matrix structure and plays important roles in cell migration, cell proliferation, and tissue repair.[21] Actin, keratin, and vimentin are constituent elements of the cytoskeleton and contribute to cell migration and morphogenesis.[22,23] These proteins have been reported to be detected in the proteomic analysis of ligamentum flavum tissue in previous studies[18,19] and the present study adds certainty to these reports.

The results of the present study suggested the biological processes occurring in the thickened ligamentum flavum, such as extracellular matrix organization, regulation of peptidase activity, extracellular matrix disassembly, and negative regulation of cell growth. Previous reports have shown that changes in the tissue mainly occur in the dorsal side of the thickened ligamentum flavum.[7,9] The load on the ligamentum flavum due to lumbar motion is higher in the dorsal side compared to the anterior side,[9] and repetitive micro-tissue damage and repair are considered a mechanism for thickening of the ligamentum flavum,[5,8] which results in scar tissue formation.[9] Some proteins found increased in the thickened ligamentum flavum in this study support this theory. Fibronectin is a glycoprotein found in the extracellular matrix, deposits during wound repair, and has a critical role in fibrogenesis.[24] HTRA1 is upregulated in keloid lesions, which are scar tissue with abnormal accumulation of extracellular matrix developing during wound healing and degradation of the keloid matrix, such as fibronectin.[25] HTRA1 also degrades decorin,[20] which is a family of small leucine-rich proteoglycans found increased in thickened ligamentum flavum tissue.[5] These proteins were also detected in the previous reports using proteomic analysis on the ligamentum flavum.[19,20] When considering other proteins that were found increased in the thickened ligamentum flavum samples, glia-derived nexin is a glycoprotein observed in a variety of cell types and is highly expressed in fibrotic tissue. Its overexpression leads to increased fibronectin.[26] Histidine-rich glycoprotein is a glycoprotein modulating angiogenesis, cell adhesion, fibroblast proliferation, and fibrinolysis, and was reported increased in pulmonary fibrosis.[27] These factors are supposed to be related to fibrosis of the ligamentum flavum, which has been considered as the main pathology of thickening of the ligamentum flavum.[9]

Chondrometaplasia is another reported pathology detected in thickened ligamentum flavum.[2,5,7] Previous reports have shown increased Type-II collagen and proteoglycans, which are cartilage matrix, in the thickened ligamentum flavum.[2,5] Some proteins found increased in the thickened ligamentum flavum in this study also included factors related to cartilage. Cartilage intermediate layer protein-2 (CLIP-2) is an extracellular matrix protein, which is mainly expressed in cartilaginous tissue.[28] Furthermore, COMP is a member of the thrombospondin family and is primarily present in cartilage.[29] These proteins have been also reported in previous reports using proteomic analysis of thickened ligamentum flavum,[19,20] and indicate the presence of chondrometaplasia. Cartilage matrix is also seen at the insertion site of the other ligaments[30] and mechanical stress is considered to cause similar change.[2] Chronic load on the ligamentum flavum due to lumbar motion may also lead to this pathology, especially on the dorsal side.

Amyloidosis is a well-known complication of long-term hemodialysis, which is derived from β2-microglobulin.[31] However, amyloid deposits in ligaments or tendons are also common, especially in elderly individuals, even without hemodialysis.[32] This type of amyloid is mostly induced by wild-type transthyretin.[33] A small number of reports have shown amyloid deposits in the ligamentum flavum of patients without hemodialysis.[32,34,35] Among those, Yanagisawa et al. reported that all LSCS patients had amyloid deposits in the ligamentum flavum, whereas the rate was 40% in the ligamentum flavum of LDH patients.[35] Furthermore, the present study showed increased protein expression of transthyretin in the thickened ligamentum flavum, which was the first time this has been reported using proteomic analysis. It was shown that the amount of amyloid deposits was correlated with ligamentum flavum thickness.[35] Increased transthyretin is supposed to indicate amyloid deposits in this study, which can be associated with thickening of the ligamentum flavum. However, increased transthyretin was observed in both dorsal and dural sides, in contrast to other pathological conditions, such as fibrosis and chondrometaplasia. Transthyretin amyloid deposition is a cause of systemic disease,[36] and the mechanism related to the thickness of the ligamentum flavum remains uncertain and should be clarified in future studies.

The limitations of this study are as follows: (1) the sample size was small and statistical analysis for proteome analysis was not conducted; (2) the average age of the LSCS group was higher than that of the LDH group; and (3) the number of upregulated proteins in the thickened ligamentum flavum was relatively small. In reference to the results of this study, further studies should be performed to confirm the pathological mechanisms suggested by this study. In addition, given that age can affect the changes occurring in the ligamentum flavum, and since LSCS patients are generally older than LDH patients, it is difficult to set a proper control group. Further, ligamentum flavum of LDH patients in this study tended to increase in thickness. Comparative high age in LDH patients in this study might make the difference between LSCS and LDH groups less significant. Furthermore, there were relatively big individual differences in each group in this study. Comparing the dorsal and anterior sides of ligamentum flavum samples can be used to assess changes occurring on the dorsal side, which can assess changes occurring in the same individuals.

5 | CONCLUSION

The present study investigated the pathology of the thickened ligamentum flavum using proteomic analysis and suggested that a

repair process via fibrosis, chondrometaplasia, and amyloid deposits were important pathologies occurring in thickened ligamentum flavum.

AUTHOR CONTRIBUTIONS

Yutaka Yabe, Yoshihiro Hagiwara, and Masahiro Tsuchiya contributed to the research design. Shinichirou Yoshida, Takahiro Onoki, and Keisuke Ishikawa collected the data. Yutaka Yabe, Takashi Minowa, Taro Takemura, and Shinya Hattori analyzed the data. Yutaka Yabe, Yoshihiro Hagiwara, and Masahiro Tsuchiya drafted the manuscript. Shinichirou Yoshida provided advice for research. All authors have read and approved the final version of the manuscript.

ACKNOWLEDGMENT

This study was supported by "Nanotechnology Platform Project" operated by the Ministry of Education, Culture, Sports, Science and Technology (MEXT), Japan (No. JPMXP09 S20NM0025).

CONFLICT OF INTEREST

The authors declare no conflicts of interest.

ORCID

Yutaka Yabe https://orcid.org/0000-0001-5875-8082

REFERENCES

1. Szpalski M, Gunzburg R. Lumbar spinal stenosis in the elderly: an overview. *Eur Spine J*. 2003;*12*(suppl 2):S170-S175.
2. Yoshida M, Shima K, Taniguchi Y, et al. Hypertrophied ligamentum flavum in lumbar spinal canal stenosis. Pathogenesis and morphologic and immunohistochemical observation. *Spine*. 1992;*17*:1353-1360.
3. Schönström NR, Hansson TH. Thickness of the human ligamentum flavum as a function of load: an in vitro experimental study. *Clin Biomech*. 1991;*6*:19-24.
4. Park JB, Lee JK, Park SJ, et al. Hypertrophy of ligamentum flavum in lumbar spinal stenosis associated with increased proteinase inhibitor concentration. *J Bone Joint Surg Am*. 2005;*87*:2750-2757.
5. Yabe Y, Hagiwara Y, Ando A, et al. Chondrogenic and fibrotic process in the ligamentum flavum of patients with lumbar spinal canal stenosis. *Spine*. 2015;*40*:429-435.
6. Altinkaya N, Yildirim T, Demir S, et al. Factors associated with the thickness of the ligamentum flavum: is ligamentum flavum thickening due to hypertrophy or buckling? *Spine*. 2011;*36*:E1093-E1097.
7. Kosaka H, Sairyo K, Biyani A, et al. Pathomechanism of loss of elasticity and hypertrophy of lumbar ligamentum flavum in elderly patients with lumbar spinal canal stenosis. *Spine*. 2007;*32*:2805-2811.
8. Yabe Y, Hagiwara Y, Tsuchiya M, et al. Decreased elastic fibers and increased proteoglycans in the ligamentum flavum of patients with lumbar spinal canal stenosis. *J Orthop Res*. 2016;*34*:1241-1247.
9. Sairyo K, Biyani A, Goel V, et al. Pathomechanism of ligamentum flavum hypertrophy: a multidisciplinary investigation based on clinical, biomechanical, histologic, and biologic assessments. *Spine*. 2005;*30*:2649-2656.
10. Sairyo K, Biyani A, Goel VK, et al. Lumbar ligamentum flavum hypertrophy is due to accumulation of inflammation-related scar tissue. *Spine*. 2007;*32*:E340-E347.
11. Hagiwara Y, Mori M, Kanazawa K, et al. Comparative proteome analysis of the capsule from patients with frozen shoulder. *J Shoulder Elbow Surg*. 2018;*27*:1770-1778.
12. Schwanhäusser B, Busse D, Li N, et al. Global quantification of mammalian gene expression control. *Nature*. 2011;*473*:337-342.
13. Hur JW, Kim BJ, Park JH, et al. The mechanism of ligamentum flavum hypertrophy: introducing angiogenesis as a critical link that couples mechanical stress and hypertrophy. *Neurosurgery*. 2015;*77*:274-281. discussion 81–82.
14. Hur JW, Bae T, Ye S, et al. Myofibroblast in the ligamentum flavum hypertrophic activity. *Eur Spine J*. 2017;*26*:2021-2030.
15. Abbas J, Hamoud K, Masharawi YM, et al. Ligamentum flavum thickness in normal and stenotic lumbar spines. *Spine*. 2010;*35*:1225-1230.
16. Witkowski C, Harkins J. Using the GELFREE 8100 fractionation system for molecular weight-based fractionation with liquid phase recovery. *J Vis Exp*. 2009;*34*:1842.
17. Little D, Thompson JW, Dubois LG, et al. Proteomic differences between male and female anterior cruciate ligament and patellar tendon. *PLoS One*. 2014;*9*:e96526.
18. Sato N, Taniguchi T, Goda Y, et al. Proteomic analysis of human tendon and ligament: solubilization and analysis of insoluble extracellular matrix in connective tissues. *J Proteome Res*. 2016;*15*:4709-4721.
19. Kamita M, Mori T, Sakai Y, et al. Proteomic analysis of ligamentum flavum from patients with lumbar spinal stenosis. *Proteomics*. 2015;*15*:1622-1630.
20. Sidon E, Shemesh SS, Mor-Yossef Moldovan L, et al. Molecular profile of ultrastructure changes of the ligamentum flavum related to lumbar spinal canal stenosis. *J Cell Biochem*. 2019;*120*:11716-11725. doi:10.1002/jcb.28451
21. Yoon JH, Halper J. Tendon proteoglycans: biochemistry and function. *J Musculoskelet Neuronal Interact*. 2005;*5*:22-34.
22. Jiu Y, Lehtimäki J, Tojkander S, et al. Bidirectional interplay between vimentin intermediate filaments and contractile actin stress fibers. *Cell Rep*. 2015;*11*:1511-1518.
23. Esue O, Carson AA, Tseng Y, et al. A direct interaction between actin and vimentin filaments mediated by the tail domain of vimentin. *J Biol Chem*. 2006;*281*:30393-30399.
24. Muro AF, Moretti FA, Moore BB, et al. An essential role for fibronectin extra type III domain a in pulmonary fibrosis. *Am J Respir Crit Care Med*. 2008;*177*:638-645.
25. Yamawaki S, Naitoh M, Kubota H, et al. HtrA1 is specifically upregulated in active keloid lesions and stimulates keloid development. *Int J Mol Sci*. 2018;*19*:1275.
26. François D, Venisse L, Marchal-Somme J, et al. Increased expression of protease nexin-1 in fibroblasts during idiopathic pulmonary fibrosis regulates thrombin activity and fibronectin expression. *Lab Invest*. 2014;*94*:1237-1246.
27. Ernst G, Dantas E, Sabatté J, et al. Histidine-rich glycoprotein and idiopathic pulmonary fibrosis. *Respir Med*. 2015;*109*:1589-1591.
28. Mori M, Nakajima M, Mikami Y, et al. Transcriptional regulation of the cartilage intermediate layer protein (CILP) gene. *Biochem Biophys Res Commun*. 2006;*341*:121-127.
29. Agarwal P, Schulz JN, Blumbach K, et al. Enhanced deposition of cartilage oligomeric matrix protein is a common feature in fibrotic skin pathologies. *Matrix Biol*. 2013;*32*:325-331.
30. Gao J, Messner K, Ralphs JR, et al. An immunohistochemical study of enthesis development in the medial collateral ligament of the rat knee joint. *Anat Embryol Berl*. 1996;*194*:399-406.
31. Inatomi K, Matsumoto T, Tomonaga T, et al. Histological analysis of the ligamentum flavum of patients with dialysis-related spondyloarthropathy. *J Orthop Sci*. 2004;*9*:285-290.
32. Sueyoshi T, Ueda M, Jono H, et al. Wild-type transthyretin-derived amyloidosis in various ligaments and tendons. *Hum Pathol*. 2011;*42*:1259-1264.

33. Gioeva Z, Urban P, Meliss RR, et al. ATTR amyloid in the carpal tunnel ligament is frequently of wildtype transthyretin origin. *Amyloid*. 2013; *20*:1-6.
34. Westermark P, Westermark GT, Suhr OB, et al. Transthyretin-derived amyloidosis: probably a common cause of lumbar spinal stenosis. *Ups J Med Sci*. 2014;*119*:223-228.
35. Yanagisawa A, Ueda M, Sueyoshi T, et al. Amyloid deposits derived from transthyretin in the ligamentum flavum as related to lumbar spinal canal stenosis. *Mod Pathol*. 2015;*28*:201-207.
36. Dowd RS, Nail TJ, Arkun K, et al. Where neurosurgery meets heart failure: a case report of a patient with amyloid transthyretin wild type in the ligamentum flavum and cardiac tissue with bilateral carpal tunnel syndrome. *World Neurosurg*. 2019;*131*: 104-107.

SUPPORTING INFORMATION

Additional supporting information may be found in the online version of the article at the publisher's website.

How to cite this article: Yabe, Y., Hagiwara, Y., Tsuchiya, M., Minowa, T., Takemura, T., Hattori, S., Yoshida, S., Onoki, T., & Ishikawa, K. (2022). Comparative proteome analysis of the ligamentum flavum of patients with lumbar spinal canal stenosis. *JOR Spine*, *5*(4), e1210. https://doi.org/10.1002/jsp2.1210